



THE UNIVERSITY *of* EDINBURGH

Edinburgh Research Explorer

Shedding light on the origin of ^{204}Pb , the heaviest s-process only isotope in the solar system

Citation for published version:

The n_TOF Collaboration, Lederer-Woods, C, Lonsdale, SJ & Woods, PJ 2024, 'Shedding light on the origin of ^{204}Pb , the heaviest s-process only isotope in the solar system', *Physical Review Letters*.

Link:

[Link to publication record in Edinburgh Research Explorer](#)

Document Version:

Peer reviewed version

Published In:

Physical Review Letters

General rights

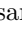
Copyright for the publications made accessible via the Edinburgh Research Explorer is retained by the author(s) and / or other copyright owners and it is a condition of accessing these publications that users recognise and abide by the legal requirements associated with these rights.

Take down policy

The University of Edinburgh has made every reasonable effort to ensure that Edinburgh Research Explorer content complies with UK legislation. If you believe that the public display of this file breaches copyright please contact openaccess@ed.ac.uk providing details, and we will remove access to the work immediately and investigate your claim.



1 Shedding light on the origin of ^{204}Pb , the heaviest s-only isotope in the solar system

2 A. Casanovas-Hoste ^{1,2,3,*} C. Domingo-Pardo,² J. Lereendegui-Marco,⁴ C. Guerrero,⁴ A. Tarifeño-Saldivia,²
3 M. Krťička,⁵ M. Pignatari,^{6,7,8,9} F. Calviño,¹ D. Schumann,¹⁰ S. Heinitz,¹⁰ R. Dressler,¹⁰ U. Köster,¹¹ O. Aberle,³
4 J. Andrzejewski,¹² L. Audouin,¹³ V. Bécarea,¹⁴ M. Bacak,¹⁵ J. Balibrea-Correa,¹⁴ M. Barbagallo,¹⁶ S. Barros,¹⁷
5 F. Bečvář,⁵ C. Beinrucker,¹⁸ E. Berthoumieux,¹⁹ J. Billowes,²⁰ D. Bosnar,²¹ M. Brugger,³ M. Caamaño,²²
6 M. Calviani,³ D. Cano-Ott,¹⁴ R. Cardella,³ D. M. Castelluccio,^{23,24} F. Cerutti,³ Y. H. Chen,¹³ E. Chiaveri,³
7 N. Colonna,¹⁶ G. Cortés,¹ M. A. Cortés-Giraldo,⁴ L. Cosentino,²⁵ L. A. Damone,^{16,26} M. Diakaki,¹⁹ E. Dupont,¹⁹
8 I. Durán,²² B. Fernández-Domínguez,²² A. Ferrari,³ P. Ferreira,¹⁷ P. Finocchiaro,²⁵ V. Furman,²⁷ K. Göbel,¹⁸
9 A. R. García,¹⁴ A. Gawlik-Ramiega,¹² T. Glodariu †,²⁸ I. F. Gonçalves,¹⁷ E. González-Romero,¹⁴ A. Goverdovski,²⁹
10 E. Griesmayer,¹⁵ F. Gunsing,^{19,3} H. Harada,³⁰ T. Heftrich,¹⁸ J. Heyse,³¹ D. G. Jenkins,³² E. Jericha,¹⁵
11 F. Käppeler †,³³ Y. Kadi,³ T. Katabuchi,³⁴ P. Kavrigin,¹⁵ V. Ketlerov,²⁹ V. Khryachkov,²⁹ A. Kimura,³⁰
12 N. Kivel,¹⁰ M. Kokkoris,³⁵ E. Leal-Cidoncha,²² C. Lederer-Woods,³⁶ H. Leeb,¹⁵ S. Lo Meo,^{23,24} S. J. Lonsdale,³⁶
13 R. Losito,³ D. Macina,³ J. Marganec,¹² T. Martínez,¹⁴ C. Massimi,^{24,37} P. Mastinu,³⁸ M. Mastro marco,¹⁶
14 F. Matteucci,^{39,40} E. A. Maugeri,¹⁰ E. Mendoza,¹⁴ A. Mengoni,²³ P. M. Milazzo,³⁹ F. Mingrone,²⁴ M. Mirea †,²⁸
15 S. Montesano,³ A. Musumarra,^{25,41} R. Nolte,⁴² A. Oprea,²⁸ N. Patronis,⁴³ A. Pavlik,⁴⁴ J. Perkowski,¹²
16 I. Porras,^{3,45} J. Praena,^{4,45} J. M. Quesada,⁴ K. Rajeev,⁴⁶ T. Rauscher,^{47,48} R. Reifarth,¹⁸ A. Riego-Perez,⁴⁹
17 Y. Romanets,¹⁷ P. C. Rout,⁴⁶ C. Rubbia,³ J. A. Ryan,²⁰ M. Sabaté-Gilarte,^{3,4} A. Saxena,⁴⁶ P. Schillebeeckx,³¹
18 S. Schmidt,¹⁸ P. Sedyshev,²⁷ A. G. Smith,²⁰ A. Stamatopoulos,³⁵ G. Tagliente,¹⁶ J. L. Tain,² L. Tassan-Got,¹³
19 A. Tsinganis,³⁵ S. Valenta,⁵ G. Vannini,^{24,37} V. Variale,¹⁶ P. Vaz,¹⁷ A. Ventura,²⁴ V. Vlachoudis,³ R. Vlastou,³⁵
20 A. Wallner,⁵⁰ S. Warren,²⁰ M. Weigand,¹⁸ C. Weiss,^{3,15} C. Wolf,¹⁸ P. J. Woods,³⁶ T. Wright,²⁰ and P. Žugec^{21,3}

(The n_TOF Collaboration)

22 ¹*Institut de Tècniques Energètiques (INTE) - Universitat Politècnica de Catalunya, Spain*

23 ²*Instituto de Física Corpuscular, CSIC - Universidad de Valencia, Spain*

24 ³*European Organization for Nuclear Research (CERN), Switzerland*

25 ⁴*Universidad de Sevilla, Spain*

26 ⁵*Charles University, Prague, Czech Republic*

27 ⁶*Konkoly Observatory, Research Centre for Astronomy and Earth Sciences (CSFK),
ELKH, H-1121, Budapest, Konkoly Thege M. út 15-17., Hungary*

28 ⁷*CSFK, MTA Centre of Excellence, Budapest, Konkoly Thege Miklós út 15-17., H-1121, Hungary*

29 ⁸*E. A. Milne Centre for Astrophysics, University of Hull, United Kingdom*

30 ⁹*NuGrid Collaboration, <http://nugridstars.org>*

31 ¹⁰*Paul Scherrer Institut (PSI), Villigen, Switzerland*

32 ¹¹*Institut Laue-Langevin (ILL), Grenoble, France*

33 ¹²*University of Lodz, Poland*

34 ¹³*Institut de Physique Nucléaire, CNRS-IN2P3, Univ. Paris-Sud,
Université Paris-Saclay, F-91191 Orsay Cedex, France*

35 ¹⁴*Centro de Investigaciones Energéticas Medioambientales y Tecnológicas (CIEMAT), Spain*

36 ¹⁵*TU Wien, Atominstytut, Stadionallee 2, 1020 Wien, Austria*

37 ¹⁶*Istituto Nazionale di Fisica Nucleare, Sezione di Bari, Italy*

38 ¹⁷*Instituto Superior Técnico, Lisbon, Portugal*

39 ¹⁸*Goethe University Frankfurt, Germany*

40 ¹⁹*CEA Irfu, Université Paris-Saclay, F-91191 Gif-sur-Yvette, France*

41 ²⁰*University of Manchester, United Kingdom*

42 ²¹*Department of Physics, Faculty of Science, University of Zagreb, Zagreb, Croatia*

43 ²²*University of Santiago de Compostela, Spain*

44 ²³*Agenzia nazionale per le nuove tecnologie (ENEA), Bologna, Italy*

45 ²⁴*Istituto Nazionale di Fisica Nucleare, Sezione di Bologna, Italy*

46 ²⁵*INFN Laboratori Nazionali del Sud, Catania, Italy*

47 ²⁶*Dipartimento Interateneo di Fisica, Università degli Studi di Bari, Italy*

48 ²⁷*Affiliated with an institute (or an international laboratory) covered by a cooperation agreement with CERN.*

49 ²⁸*Horia Hulubei National Institute of Physics and Nuclear Engineering, Romania*

50 ²⁹*Institute of Physics and Power Engineering (IPPE), Obninsk, Russia*

51 ³⁰*Japan Atomic Energy Agency (JAEA), Tokai-Mura, Japan*

52 ³¹*European Commission, Joint Research Centre (JRC), Geel, Retieseweg 111, B-2440 Geel, Belgium*

53 ³²*University of York, United Kingdom*

54 ³³*Karlsruhe Institute of Technology, Campus North, IKP, 76021 Karlsruhe, Germany*

55 ³⁴*Tokyo Institute of Technology, Japan*

56

³⁵*National Technical University of Athens, Greece*

³⁶*School of Physics and Astronomy, University of Edinburgh, United Kingdom*

³⁷*Dipartimento di Fisica e Astronomia, Università di Bologna, Italy*

³⁸*Istituto Nazionale di Fisica Nucleare, Sezione di Legnaro, Italy*

³⁹*Istituto Nazionale di Fisica Nucleare, Sezione di Trieste, Italy*

⁴⁰*Dipartimento di Astronomia, Università di Trieste, Italy*

⁴¹*Dipartimento di Fisica e Astronomia, Università di Catania, Italy*

⁴²*Physikalisch-Technische Bundesanstalt (PTB), Bundesallee 100, 38116 Braunschweig, Germany*

⁴³*University of Ioannina, Greece*

⁴⁴*University of Vienna, Faculty of Physics, Vienna, Austria*

⁴⁵*University of Granada, Spain*

⁴⁶*Bhabha Atomic Research Centre (BARC), India*

⁴⁷*Centre for Astrophysics Research, University of Hertfordshire, United Kingdom*

⁴⁸*Department of Physics, University of Basel, Switzerland*

⁴⁹*Universitat Politècnica de Catalunya, Spain*

⁵⁰*Australian National University, Canberra, Australia*

(Dated: June 14, 2024)

Asymptotic giant branch stars are responsible for the production of most of the heavy isotopes beyond Sr observed in the solar system. Among them, isotopes shielded from the r -process contribution by their stable isobars are defined as s -only nuclei. For a long time the abundance of ^{204}Pb , the heaviest s -only isotope, has been a topic of debate because state-of-the-art stellar models appeared to systematically underestimate its solar abundance. Besides the impact of uncertainties from stellar models and galactic chemical evolution simulations, this discrepancy was further obscured by rather divergent theoretical estimates for the neutron capture cross section of its radioactive precursor in the neutron-capture flow, ^{204}Tl ($t_{1/2} = 3.78$ years), and by the lack of experimental data on this reaction. We present the first ever neutron capture measurement on ^{204}Tl , conducted at the CERN neutron time-of-flight facility n_TOF, employing a sample of only 9 mg of ^{204}Tl produced at the ILL high flux reactor. By complementing our new results with semi-empirical calculations we obtained, at the s -process temperatures of $kT \approx 8$ keV and $kT \approx 30$ keV, maxwellian-averaged cross sections (MACS) of 580(168) mb and 260(90) mb, respectively. These figures are about 3% lower and 20% higher than the corresponding values widely used in astrophysical calculations, which were based only on theoretical calculations. By using the new ^{204}Tl MACS, the uncertainty arising from the $^{204}\text{Tl}(n, \gamma)$ cross section on the s -process abundance of ^{204}Pb has been reduced from $\sim 30\%$ down to $+8/-6\%$, and the s -process calculations are in agreement with the latest solar system abundance of ^{204}Pb reported by K. Lodders in 2021.

Since the observation of technetium in the stellar atmosphere of R-Andromedae [1] and the emergence of the subsequent theory of synthesis of elements in stars [2, 3], the study of Asymptotic Giant Branch (AGB) stars has played an important role in disentangling the origin of the elements beyond iron. Indeed, due to the activation of the slow neutron-capture process (s process), AGB stars are one of the main sources of nuclei heavier than Sr [4–6]. The solar isotopic composition is the best known abundance distribution, and it is a crucial benchmark to study the galactic chemical evolution (GCE) of the Milky Way [7–9]. In particular, the isotopic pattern of heavy elements is derived mainly from Ivuna-type carbonaceous (CI) chondrites analysis, and its precise measurement is a very active field of research [10]. This pattern is the result of GCE driven by multiple generations of stars and different nucleosynthesis mechanisms. However, it is possible to identify nuclei that are produced almost entirely by the s process, since they are shielded from contributions of the rapid neutron-capture process (r process), which is the other main mechanism contributing to the formation of heavy nuclei [11]. These so-called s -only isotopes play a pivotal role in studying the s -process nucleosynthesis in AGB stars and in validating stellar models at different metallicities [7, 12–15]. ^{204}Pb is the heaviest s -only isotope and thus it serves to benchmark state-of-the-art AGB models in the heavy-mass region around neutron magic number $N = 126$, corresponding to the s -process peak in the Pb-Bi region. Also, ^{204}Pb is the single lead isotope that preserves its primordial abundance, thus enabling the Pb-Pb chronometry of the early Solar System [16, 17]. As it can be inferred from Figure 1 the production of ^{204}Pb is directly affected by the interplay between the β^- -decay rate and the neutron capture cross section of the unstable ^{204}Tl ($t_{1/2} = 3.78$ y), which acts as a branching point in the s process path. Until now, apart from a transmission measurement from 1968 [18] in the 0.2 eV to 1 keV energy range, only theoretical calculations of the Maxwellian-averaged cross section (MACS) of $^{204}\text{Tl}(n, \gamma)$ were available [19]. The latter differ from each other by more than a factor of two at $kT=30$ keV, i.e. from 97 mb [20] to the value of 224(78) mb estimated by TENDL-2021 [21]. An estimation of 134 ± 40 mb was obtained from the interpolation of time-of-flight (TOF) measurements of the neighbouring isotopes ^{203}Tl and ^{205}Tl at ORNL [22]. Finally, the value of 215 ± 38 mb

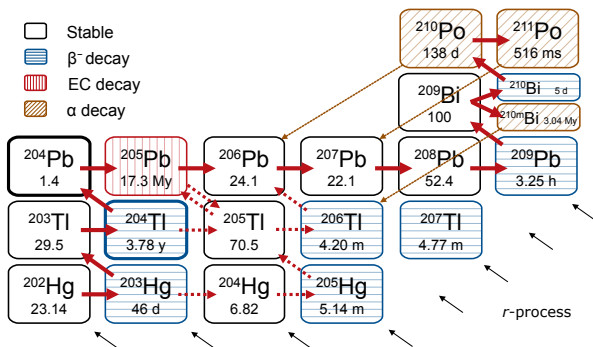


FIG. 1. Schematic view of the chart of nuclei at the termination of the s -process. The arrows correspond to the main s process path, with dashed arrows depicting paths strongly enhanced during high temperature and high neutron density events.

recommended by the KADoNiS v0.3 database [19], commonly used as reference for nucleosynthesis calculations, corresponds to a previous theoretical calculation by Bao *et al.* obtained with the NON-SMOKER code [23]. Note that the uncertainty of 18% quoted there is rather questionable in view of the large discrepancies among different theoretical estimates [19].

Previous nucleosynthesis calculations based on the KADoNiS v0.3 ^{204}Tl MACS found a systematic underproduction of the solar abundance of ^{204}Pb [12, 14, 15, 24]. Some of the missing ^{204}Pb could have been produced by the γ process in supernovae [25–27]. However, the origin of this process in stars is still matter of debate and its GCE contribution to ^{204}Pb still remains rather uncertain [28]. Another possible explanation of the predicted deficiency could be a yet unidentified fractionation mechanism operating in the early solar system. By comparing the observed solar abundances with nearby solar twins, Gonzalez[29] suggested the corrections to the elemental meteoritic abundances needed to take this effect into account. For the case of Pb, this led to a reduction of the Pb/Sm elemental ratio of $\log_{10}(\text{Pb}/\text{Sm}) = -0.1$.

As described by Bisterzo *et al.* [15], a reliable assessment of additional nucleosynthesis contributions to ^{204}Pb from other stellar sources and/or fractionation effects has been hindered by the uncertainty in the thermal dependency of the β^- -decay rate [30, 31], and most importantly, by the large uncertainty in the neutron capture cross section of ^{204}Tl and the lack of experimental data.

However, direct measurements on radioactive isotopes are very challenging. When the reaction product is stable and thus the sensitive activation technique can not be applied, the TOF technique represents the only alternative. Thus far, from the 21 key s -process branching nuclei discussed by Käppeler *et al.* [5], it has been successfully applied only to ^{63}Ni [32], ^{79}Se [33], ^{151}Sm [34] and ^{171}Tm [35]. Of these nuclei only the last has a very short half-life (1.92 y) comparable to that of ^{204}Tl .

In this work, the ^{204}Tl sample was produced from a machine-pressed pellet of Tl_2O_3 containing 225 mg of thallium, enriched up to 99.5% in ^{203}Tl . This pellet was irradiated for 55 days in the high flux reactor of the Institute Laue Langevin (ILL). From the initial seed composition and the irradiation parameters, the content of ^{204}Tl at the time of the experiment was calculated to be 9.0(5) mg, corresponding to an enrichment of 4.0(2)%. Prior to the irradiation at ILL, the pellet had been enclosed in a sealed quartz capsule in order to avoid any loss of material. The capsule was cylindrical in shape, with a length of 30 mm, an external diameter of 8 mm, and 1 mm thick walls.

The capture experiment was performed at the CERN neutron time-of-flight facility, n-TOF [36]. At n-TOF pulses of neutrons are produced by the spallation reactions induced by a 20 GeV/c proton beam impinging a massive lead target, with the neutron energy E_n determined by applying the TOF technique. The experiment was conducted at the 185 m neutron beam line of the Experimental Area 1 (EAR1). This beam line offers the best combination among all current world TOF facilities in terms of high instantaneous neutron flux and long flight path [37], which allows to achieve a resolution of $\Delta E_n/E_n = 10^{-3}$ or better in the E_n range between 1 eV and 10 keV [36].

The neutron capture yield was measured by detecting the prompt de-excitation γ -rays emitted after each capture event, employing the n-TOF standard setup of four C_6D_6 liquid scintillation detectors [38], which are optimized to minimize their neutron sensitivity [39]. Lead foils were placed on the detectors to reduce the impact of the low energy bremsstrahlung γ -rays arising from the ^{204}Tl decay. The γ -ray cascade detection efficiency was rendered proportional to the total energy of the cascade E_C , and thus independent of the particular de-excitation path of the cascade, by applying the Pulse Height Weighting Technique (PHWT) [40–42]. The application of the PHWT required detailed MC simulations of the detection setup response to a wide range of γ -ray energies, performed with the Geant4 toolkit [43–45]. After applying the PHWT, the experimental capture yield can be expressed as

$$Y_{\text{exp}}(E_n) = f_{\text{th}} \cdot f_N \cdot \frac{C_w(E_n) - B_w(E_n)}{\phi(E_n) \cdot E_C}. \quad (1)$$

Here, $C_w(E_n)$ and $B_w(E_n)$ are the weighted total and background counts, respectively, while $\phi(E_n)$ is the neutron fluence, derived from the energy dependence of the n-TOF neutron flux [46].

The background counts, $B_w(E_n)$, had two dominant components, which were assessed separately. The counts generated by the activity of the sample were evaluated by acquiring data with the sample and without neutron beam. The second, *beam induced background* component, mostly originating from the capture of beam neutrons

scattered mainly by the sample quartz container, was evaluated by measuring an identical empty container.

The absolute normalization factor, f_N , accounts for the fraction of beam intersecting the sample. For the ^{204}Tl -enriched sample the determination of f_N required to consider the spatial distribution of activated material inside the capsule and thus, f_N was obtained in a two-step process. First, a separate measurement using a highly enriched ^{203}Tl sample was conducted to determine the capture area A_r of $^{203}\text{Tl}(n, \gamma)$ resonances. A_r is defined as [47]

$$A_r = 2\pi^2 \lambda_n^2 g_J \frac{\Gamma_n \Gamma_\gamma}{\Gamma_n + \Gamma_\gamma}, \quad (2)$$

where $\lambda = \lambda/2\pi$ is the reduced de Broglie wave length of the neutron, g_J is the resonance spin factor, Γ_γ and Γ_n are the radiative and the neutron widths, respectively.

Because mass and geometry were precisely known for the ^{203}Tl sample, the $^{203}\text{Tl}(n, \gamma)$ yield could be determined accurately by applying the conventional saturated resonance method using the well-known 4.9 eV resonance in ^{197}Au [48, 49], and the fact that the neutron flux of n_TOF EAR1 is known with an accuracy of 2% or better in the energy range between 1 eV and 10 keV [46]. Further details of the experimental setup and the analysis results for the $^{203}\text{Tl}(n, \gamma)$ measurement will be given in a separate publication [50].

Afterwards, f_N could be obtained for the ^{204}Tl -enriched sample by fixing the A_r of the newly measured four strongest ^{203}Tl resonances, which featured prominently in the yield due to the dominant content (96%) of ^{203}Tl .

Lastly, f_{th} in Eq. (1) accounts for the part of the capture spectrum missing under the pulse-height detection threshold, and it was calculated from MC simulations of the de-excitation cascades of $^{197}\text{Au}(n, \gamma)$, $^{203}\text{Tl}(n, \gamma)$ and $^{204}\text{Tl}(n, \gamma)$ [51]. Despite the relatively high threshold of 600 keV, necessary to reduce further the bremsstrahlung background arising from the ^{204}Tl β^- -decay, the corresponding correction factors were less than 3% owing to the similarity in pulse-height spectra between the two Tl isotopes and gold.

For all samples, the resonance parameters were determined by analyzing Y_{exp} with the Bayesian R-Matrix code SAMMY [52]. Once the normalization procedure was applied, a capture yield for $^{204}\text{Tl}(n, \gamma)$ could be obtained via Eq. (1). The ^{204}Tl enrichment and its associated uncertainty were evaluated by fitting the concentration of the daughter ^{204}Pb in the experimental yield, using the strongest resonance of ^{204}Pb and the corresponding parameters from Ref. [53].

A total systematic uncertainty of 12% was estimated for the experimental $^{204}\text{Tl}(n, \gamma)$ MACS calculated from resonances directly measured; partial contributions are summarized in Table II in the Supplemental Material.

The R-Matrix analysis allowed to identify eleven $^{204}\text{Tl}(n, \gamma)$ resonances, all below $E_n = 4$ keV. A problem is that higher E_n are involved in s -process nucleosynthesis in low mass AGB stars. Most of the neutrons are produced by the $^{13}\text{C}(\alpha, n)^{16}\text{O}$ reaction in the radiative ^{13}C pocket, in the upper part of the He intershell region, at temperatures corresponding to thermal energies of $kT \approx 8$ keV. A smaller amount of neutrons are also released by the partial activation of the $^{22}\text{Ne}(\alpha, n)^{25}\text{Mg}$ reaction at the bottom of the He intershell, where $kT \approx 25 - 30$ keV is reached during the recurrent convective Thermal Pulse (TP) events triggered by He fusion [6, 54, 55]. During TPs, the $^{22}\text{Ne}(\alpha, n)^{25}\text{Mg}$ may generate neutron densities in the order of $n_n \sim 10^{10-11} \text{ cm}^{-3}$ (orders of magnitude higher than in the ^{13}C pocket), and allows to open several branching points along the s -process path [15, 56, 57].

To extend the MACS up to $kT \approx 30$ keV a methodology similar to that described in [35] was applied. From new average resonance parameters determined in the present experiment, and the simulation of random resonance sequences, the fraction of the total MACS at higher kT energies that could be measured in our experiment was determined.

Combining these calculated fractions with the directly measured contributions, the total MACS at each kT energy was determined including its uncertainty. Further details on the procedure, the determination of average parameters and the evaluation of the MACS uncertainty are provided in the Supplemental Material.

The total MACS as a function of kT is shown in Figure 2. We obtained values of 580(168) mb and 260(90) mb at $kT = 8$ keV and 30 keV, respectively (see the Supplemental Material for the values at other kT). Note that the observable contribution corresponds to about 25% in the first case, and 5% in the latter. The expected value of the total MACS at $kT = 30$ keV is about 20% higher than the KADoNiS v0.3 recommended value of 215 mb from Bao *et al.*. The theoretical expected values of 175 mb from Rauscher and Thielemann [58] and 221 mb from TENDL-2021 [21] remain compatible within the quoted uncertainty. This is not the case for the values calculated by Harris (97 mb) [20] and Macklin (124 mb) [22]. In Figure 2 the shadowed region is used to represent the range of previous theoretical estimations, with the upper bound defined by TENDL-2021 and the lower bound by the value of Harris at 30 keV and its extrapolation to other kT by employing the energy dependence of TENDL-2021. The cross symbol corresponds to the values by Bao *et al.* [23].

To study the impact of the new ^{204}Tl MACS in the production of ^{204}Pb - s -process nucleosynthesis calculations were performed using NuGrid post-processing codes applied to AGB stellar evolution simulations from MESA [59, 60]. Our calculations, in which only the $^{204}\text{Tl}(n, \gamma)$ cross section was varied, included the simulations of the

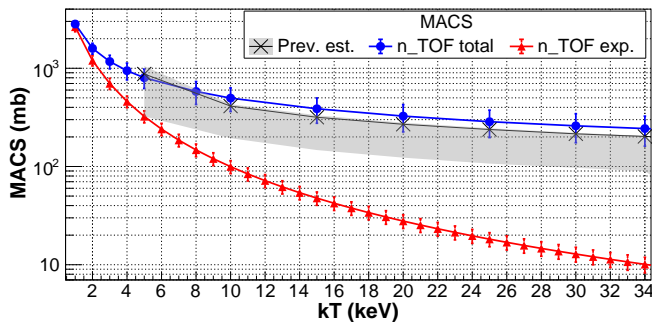


FIG. 2. MACS as a function of thermal energy (kT). Red solid triangles correspond to the contribution of observed resonances, whereas the blue solid circles represent the total MACS obtained in this work. The gray shadowed region indicates the range covered by previous theoretical estimations (see text for details), with the cross highlighting the calculation by Bao *et al.* [23].

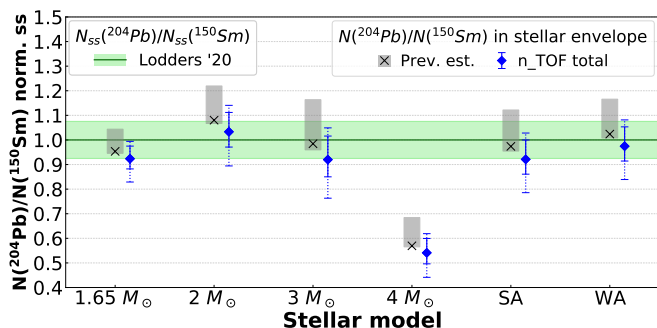


FIG. 3. Isotopic abundance ratios $N(^{204}\text{Pb})/N(^{150}\text{Sm})$ in the star envelope at the end of the AGB phase, obtained using the MACS from Figure 2 for the stellar models described in the text. All values are normalized to the solar system (ss) ratio [10], which is highlighted by the thick green bar with the green shaded band depicting its uncertainty. Solid error bars reflect only the uncertainty contribution from the cross section, while dashed error bars include also the uncertainty on the thermal dependency of the β^- -decay of ^{204}Tl [31].

320 full AGB stage for stars with initial masses 1.65, 2, 3
 321 and $4 M_{\odot}$, all with metallicity $Z = 0.006$, which approx-
 322 imately corresponds to between one half and one third of
 323 the present value [10, 61, 62]. It is worth noting that al-
 324 though the present solar system s -process abundances are
 325 the outcome of the contribution of multiple generations
 326 of stars of different masses and metallicities [7, 8, 14, 24],
 327 GCE calculations have confirmed that the dominant contribu-
 328 tion to ^{204}Pb comes from the so-called *main* compo-
 329 nent of the s process originating from low-mass AGB
 330 stars in the mass range of 1.5 to $3 M_{\odot}$, with a minor con-
 331 tribution of only 2% expected from very low metallicity
 332 ($Z < 0.001$) AGB stars [7].

333 Hence, a more representative description of the main
 334 s -process abundances was obtained by calculating a
 335 weighted average (WA) of the 1.65, 2 and $3 M_{\odot}$ NuGrid

336 yields, applying the weights obtained from Salpeter's ini-
 337 tial mass function (IMF) [63]. The weights assigned to
 338 each of the NuGrid models corresponded, respectively, to
 339 the fraction of stars between 1.5 and $1.8 M_{\odot}$, between 1.8
 340 and $2.5 M_{\odot}$, and between 2.5 and $3.5 M_{\odot}$, all normalized
 341 to the integral between 1.5 and $3.5 M_{\odot}$.

342 The value of the WA was also compared to the sim-
 343 ple average (SA) of the production yields of 1.65 and 3
 344 M_{\odot} AGB stars of half-solar metallicity, similar to the
 345 approach employed in the past to reproduce s -process
 346 abundances [12, 15]. Note that no significant differences
 347 are expected in terms of s -process nucleosynthesis when
 348 using $1.65 M_{\odot}$ instead of the $1.5 M_{\odot}$ employed in [12].
 349 To directly compare the calculated s -process yields with
 350 the solar s -only abundances, the ^{204}Pb yields are normal-
 351 ized to the production of the unbranched s -only isotope
 352 ^{150}Sm . This normalization is commonly used to directly
 353 compare s -process nucleosynthesis calculations with solar
 354 abundances [15, 24, 56]. Here, the use of the ratio
 355 $\rho_N = N(^{204}\text{Pb})/N(^{150}\text{Sm})$ allow one to have a prelimi-
 356 nary estimate about the impact of the new MACS on the
 357 expected s -process production of ^{204}Pb before perform-
 358 ing more detailed GCE calculations. Indeed, by means
 359 of this ratio the impact of some of the stellar physics and
 360 nuclear uncertainties equally affecting the production of
 361 both ^{150}Sm and ^{204}Pb can be minimized [15].

362 Figure 3 shows the ratio ρ_N in the star envelope at
 363 the end of the AGB stage for the individual stars and
 364 for the two averaged combinations. Uncertainties were
 365 obtained by averaging correspondingly those of the separ-
 366 ate stellar models. ρ_N was obtained for the MACS from
 367 this work and also for previous calculations by Harris
 368 [20], Rauscher and Thielemann [58], Bao *et al.* [23] and
 369 TENDL-2021 [21]. For simplicity, all calculated ratios
 370 have been normalized to the expected value of the ratio
 371 in the solar system of Lodders [10], which is derived from
 372 CI-chondrites.

373 The MACS from this work yields a solar system nor-
 374 malized ratio $\rho_N = 0.97(+8, -6)$ for the WA, which is in
 375 agreement with Lodders without the need of additional
 376 contributions to ^{204}Pb .

377 We have also evaluated the impact of the uncertainty
 378 in the thermal dependency of the β^- -decay rate of ^{204}Tl
 379 at stellar temperatures, for which we performed addi-
 380 tional calculations with our MACS and the minimum
 381 and maximum β^- -decay rates provided by [31]. By sum-
 382 ming the MACS and the β^- -decay uncertainties, we ob-
 383 tained a total uncertainty range for the normalized ρ_N of
 384 $(+14\%, -11\%)$ for the WA. Note that future experiments
 385 like PANDORA [64] could provide valuable experimental
 386 constraints to this rate. The uncertainty in the thermal
 387 dependency for the much less frequent decay of ^{204}Tl to
 388 ^{204}Hg produced a negligible variation ($< 0.3\%$) in the
 389 final abundance of ^{204}Pb .

390 It is important to remark that the ^{204}Pb production
 391 (and therefore the $^{204}\text{Pb}/^{150}\text{Sm}$ ratio) becomes sensitive

392 to the neutron density and the temperature conditions
 393 during the TP episodes which, in turn, influence the
 394 interplay between the MACS of ^{204}Tl and its temperature-
 395 dependent β^- -decay at this s -process branching.

396 In these conditions, some differences arising from the
 397 new ^{204}Tl MACS may be expected comparing different
 398 AGB stellar models. For instance, the choice of including
 399 convective-boundary mixing at the bottom of TPs [59]
 400 makes the He intershell in AGB models a bit hotter than
 401 other models without such a feature [65, 66]. Among
 402 other things, this will affect the activation of s -process
 403 branchings, including ^{204}Tl [13]. The models shown in
 404 Figure 3 can be used to gain some insight into these as-
 405 pects. In comparison to the $3 M_{\odot}$ star, the $1.65 M_{\odot}$
 406 model reaches lower TP temperatures. Thus, once the
 407 s -process path reaches ^{204}Tl lower neutron densities and
 408 capture rates are obtained with respect to the competing
 409 β -decay channel. This leads to a smaller spread in the
 410 $^{204}\text{Pb}/^{150}\text{Sm}$ ratio among different $^{204}\text{Tl}(n, \gamma)$ cross sec-
 411 tion values in the $1.65 M_{\odot}$ model (see Figure 3). There-
 412 fore, the final $^{204}\text{Pb}/^{150}\text{Sm}$ production ratio becomes sensi-
 413 tive to the different state-of-the-art AGB stellar sets.
 414 Hence, it would be of interest to perform similar calcula-
 415 tions adopting the new ^{204}Tl MACS and its uncertainty
 416 with different AGB models [15, 65–67].

417 Another important uncertainty directly affecting the
 418 neutron density is the cross section of $^{22}\text{Ne}(\alpha, n)^{25}\text{Mg}$.
 419 Presently, several experimental efforts are indeed focused
 420 on the determination of both reactions cross sections [68–
 421 71]. It is worth noting that some recent recommendations
 422 by Ota *et al.* [72] and Adsley *et al.* [68] based on recent
 423 data [73, 74], apparently point to a $^{22}\text{Ne}(\alpha, n)^{25}\text{Mg}$ cross
 424 section considerably lower than previous evaluations, in-
 425 cluding the one used in this work [75]. However, the new
 426 values are not generally accepted yet [76] and additional
 427 underground experiments [77] are expected to address
 428 this discrepancies.

429 To conclude, the neutron capture cross section of the
 430 s -process branching nucleus ^{204}Tl has been measured for
 431 the first time at energies relevant for nucleosynthesis in
 432 AGB stars. The high thermal neutron flux of ILL and
 433 the high resolution and luminosity of CERN n_TOF were
 434 key to produce a sufficient amount of ^{204}Tl and to re-
 435 solve several $^{204}\text{Tl}(n, \gamma)$ resonances, respectively. New
 436 AGB nucleosynthesis calculations based on the MACS
 437 reported here are fully consistent with the observed solar
 438 abundance of ^{204}Pb and provide a more stringent con-
 439 straint on its s -process contribution. Further insight on
 440 other possible contributions to the abundance of ^{204}Pb
 441 would require a corresponding improvement in the MACS
 442 of ^{204}Tl down to a level of about 10%, which would lead
 443 to a few percent uncertainty on the isotopic abundance
 444 of ^{204}Pb . Within the present experimental uncertain-
 445 ties, there is no need to invoke additional nucleosynthesis
 446 mechanisms or fractionation effects discussed previously
 447 in the literature in order to explain the ^{204}Pb abundance

448 observed in the solar system.

449 ACKNOWLEDGEMENTS

450 We acknowledge the suggestions of three referees,
 451 which helped to improve the present article in several
 452 relevant aspects. We would like to acknowledge the fi-
 453 nancial support by the Argos Scholarship of the Univer-
 454 sitat Politècnica de Catalunya (UPC) and the Consejo
 455 de Seguridad Nuclear (CSN), by the Spanish Government
 456 Ministries MINECO (projects FPA2014-52823-C2-1/2-
 457 P and FPA2017-83946-C2-1/2-P) and MCIU (projects
 458 PID2019-104714GB-C21 and PID2022-138297NB-C21)
 459 by the EC FP7 projects NeutAndalus (Grant No.
 460 334315) and CHANDA (Grant No. 605203), and by
 461 the n_TOF Collaboration and the Institut de Tècniques
 462 Energètiques (INTE) of the UPC. A.C.H. also recog-
 463 nizes the support from a Margarita Salas grant by the
 464 UPC (Agreement CG/2021/03/23) and the Ministerio
 465 de Universidades (Order UNI/551/2021). A.C.H. and
 466 C.D.P. acknowledge support from ERC Consolidator
 467 Grant HYMNS, Grant Agreement Nr. 681740. M.P.
 468 acknowledges significant support to NuGrid from STFC
 469 (through the University of Hull’s Consolidated Grant
 470 ST/R000840/1), from the ERC Consolidator Grant
 471 (Hungary) funding scheme (Project RADIOSTAR, G.A.
 472 n. 724560), from the ChETEC COST Action (CA16117),
 473 supported by the European Cooperation in Science and
 474 Technology, from the IReNA network supported by NSF
 475 AccelNet, from the National Science Foundation (NSF,
 476 USA) under grant No. PHY-1430152 (JINA Center for
 477 the Evolution of the Elements), from the ”Lendulet-
 478 2014” Program of the Hungarian Academy of Sciences
 479 (Hungary), and from the European Union’s Horizon 2020
 480 research and innovation programme (ChETEC-INFRA –
 481 Project no. 101008324). M.P. also acknowledges the
 482 access to *viper*, the University of Hull High Perform-
 483 ance Computing Facility. C.L.W. acknowledges sup-
 484 port from the Science and Technology Facilities Council
 485 UK (ST/M006085/1), and the European Reseach Coun-
 486 cil ERC-2015-STG Nr. 677497. A support of all funding
 487 agencies of the n_TOF participating institutes is acknowl-
 488 edged.

489 * Corresponding author: adria.casanovas@upc.edu

- 490 [1] P. W. Merrill, *Astrophys. J.* **116**, 21 (1952).
 491 [2] E. M. Burbidge, G. R. Burbidge, W. A. Fowler, and
 492 F. Hoyle, *Rev. Mod. Phys.* **29**, 547 (1957).
 493 [3] A. G. W. Cameron, *Stellar evolution, nuclear astro-*
 494 *physics, and nucleogenesis. Second edition*, Tech. Rep.
 495 (1957).
 496 [4] M. Busso, R. Gallino, and G. J. Wasserburg, **37**, 239
 497 (1999).

- [5] F. Käppeler, R. Gallino, S. Bisterzo, and W. Aoki, *Rev. Mod. Phys.* **83**, 157 (2011).
- [6] A. I. Karakas and J. C. Lattanzio, **31**, e030 (2014), arXiv:1405.0062 [astro-ph.SR].
- [7] C. Travaglio, R. Gallino, M. Busso, and R. Gratton, *Astrophys. J.* **549**, 346 (2001).
- [8] N. Prantzos, C. Abia, M. Limongi, A. Chieffi, and S. Cristallo, **476**, 3432 (2018), arXiv:1802.02824 [astro-ph.GA].
- [9] C. Kobayashi, A. I. Karakas, and M. Lugaro, *Astrophys. J.* **900**, 179 (2020), arXiv:2008.04660 [astro-ph.GA].
- [10] K. Lodders, *Space Sci. Rev.* **217**, 44 (2021).
- [11] J. J. Cowan, C. Sneden, J. E. Lawler, A. Aprahamian, M. Wiescher, K. Langanke, G. Martínez-Pinedo, and F.-K. Thielemann, *Rev. Mod. Phys.* **93**, 015002 (2021).
- [12] C. Arlandini, F. Käppeler, K. Wisshak, R. Gallino, M. Lugaro, M. Busso, and O. Straniero, *Astrophys. J.* **525**, 886 (1999).
- [13] M. Lugaro, F. Herwig, J. C. Lattanzio, R. Gallino, and O. Straniero, *Astrophys. J.* **586**, 1305 (2003), arXiv:astro-ph/0212364 [astro-ph].
- [14] S. Bisterzo, C. Travaglio, R. Gallino, M. Wiescher, and F. Käppeler, *Astrophys. J.* **787**, 10 (2014), arXiv:1403.1764 [astro-ph.SR].
- [15] S. Bisterzo, R. Gallino, F. Käppeler, M. Wiescher, G. Imbriani, O. Straniero, S. Cristallo, J. Görres, and R. J. deBoer, *Mon. Not. R. Astron. Soc.* **449**, 506 (2015), arXiv:1507.06798 [astro-ph.SR].
- [16] J. N. Connelly, M. Bizzarro, A. N. Krot, Åke Nordlund, D. Wielandt, and M. A. Ivanova, *Science* **338**, 651 (2012), <https://www.science.org/doi/pdf/10.1126/science.1226919>.
- [17] J. Connelly, J. Bollard, and M. Bizzarro, *Geochim. Cosmochim. Acta* **201**, 345 (2017), isotopic studies of planetary and nuclear materials: A scientific tribute to Ian Douglass Hutcheon (1947-2015).
- [18] T. Watanabe, G. E. Stokes, and R. P. Schuman, pp 893-6 of *Neutron Cross Sections and Technology*. Goldman, D. T. (ed.). Washington, D. C., National Bureau of Standards, 1968. (1969).
- [19] I. Dillmann, M. Heil, F. Käppeler, R. Plag, T. Rauscher, and F. Thielemann, *AIP Conference Proceedings* **819**, 123 (2006), <http://www.kadonis.org>.
- [20] M. J. Harris, *Astrophys. Space Sci.* **77**, 357 (1981).
- [21] A. Koning, D. Rochman, J.-C. Sublet, N. Dzysiuk, M. Fleming, and S. van der Marck, *Nucl. Data Sheets* **155**, 1 (2019).
- [22] R. L. Macklin and R. R. Winters, *Astrophys. J.* **208**, 812 (1976).
- [23] Z. Bao, H. Beer, F. Käppeler, F. Voss, K. Wisshak, and T. Rauscher, *At. Data Nucl. Data Tables* **76**, 70 (2000).
- [24] S. Cristallo, C. Abia, O. Straniero, and L. Piersanti, *Astrophys. J.* **801**, 53 (2015), arXiv:1501.00544 [astro-ph.SR].
- [25] T. Rauscher, A. Heger, R. D. Hoffman, and S. E. Woosley, *Astrophys. J.* **576**, 323 (2002), arXiv:astro-ph/0112478 [astro-ph].
- [26] T. Rauscher, N. Dauphas, I. Dillmann, C. Fröhlich, Z. Fülöp, and G. Gyürky, *Reports on Progress in Physics* **76**, 066201 (2013), arXiv:1303.2666 [astro-ph.SR].
- [27] M. Pignatari, K. Göbel, R. Reifarth, and C. Travaglio, *International Journal of Modern Physics E* **25**, 1630003-232 (2016), arXiv:1605.03690 [astro-ph.SR].
- [28] C. Travaglio, T. Rauscher, A. Heger, M. Pignatari, and C. West, *Astrophys. J.* **854**, 18 (2018), arXiv:1801.01929 [astro-ph.SR].
- [29] G. Gonzalez, *Mon. Not. R. Astron. Soc. Lett.* **443**, L99 (2014), <https://academic.oup.com/mnras/article-pdf/443/1/L99/9420491/slu083.pdf>.
- [30] K. Takahashi and K. Yokoi, *At. Data Nucl. Data Tables* **36**, 375 (1987).
- [31] S. Goriely, *Astron. Astrophys.* **342**, 881 (1999).
- [32] C. Lederer *et al.* (n_TOF Collaboration), *Phys. Rev. Lett.* **110**, 022501 (2013).
- [33] Lerendegui-Marco, J. *et al.*, *EPJ Web Conf.* **279**, 13001 (2023).
- [34] S. Marrone *et al.* (n_TOF Collaboration), *Phys. Rev. C* **73**, 034604 (2006).
- [35] C. Guerrero *et al.* (n_TOF Collaboration), *Phys. Rev. Lett.* **125**, 142701 (2020).
- [36] C. Guerrero *et al.* (The n_TOF Collaboration), *Eur. Phys. J. A* **49**, 27 (2013).
- [37] N. Colonna, F. Gunsing, and F. Käppeler, *Prog. Part. Nucl. Phys.* **101**, 177 (2018).
- [38] J. Lerendegui-Marco *et al.* (n_TOF Collaboration), *Phys. Rev. C* **97**, 024605 (2018).
- [39] R. Plag, M. Heil, F. Käppeler, P. Pavlopoulos, R. Reifarth, and K. Wisshak, *Nucl. Instrum. Methods Phys. Res., Sect. A* **496**, 425 (2003).
- [40] R. L. Macklin and J. H. Gibbons, *Phys. Rev.* **159**, 1007 (1967).
- [41] J. L. Taín *et al.*, *J Nucl Sci Technol* **39**, 689 (2002), <https://doi.org/10.1080/00223131.2002.10875193>.
- [42] U. Abbondanno *et al.* (n_TOF Collaboration), *Nucl. Instrum. Methods Phys. Res., Sect. A* **521**, 454 (2004).
- [43] S. Agostinelli *et al.*, *Nucl. Instrum. Methods Phys. Res., Sect. A* **506**, 250 (2003).
- [44] J. Allison *et al.*, *IEEE T. Nucl. Sci.* **53**, 270 (2006).
- [45] J. Allison *et al.*, *Nucl. Instrum. Methods Phys. Res., Sect. A* **835**, 186 (2016).
- [46] M. Barbagallo *et al.* (The n_TOF Collaboration), *Eur. Phys. J. A* **49**, 156 (2013).
- [47] S. F. Mughabghab, *Atlas of Neutron Resonances (Sixth Edition)* (Elsevier, 2018).
- [48] R. L. Macklin, J. Halperin, and R. R. Winters, *Nucl. Instrum. Methods* **164**, 213 (1979).
- [49] C. Massimi *et al.* (n_TOF Collaboration), *Phys. Rev. C* **81**, 044616 (2010).
- [50] A. Casanovas *et al.*, in preparation.
- [51] A. Casanovas-Hoste, *Neutron capture cross section measurement of the heaviest s-process branching ^{204}Tl and of ^{203}Tl at CERN n_TOF*, Ph.D. thesis (2020).
- [52] N. M. Larson, *Updated User's Guide for Sammy: Multi-level R-Matrix Fits to Neutron Data Using Bayes' Equations*, Tech. Rep. (Oak Ridge National Laboratory, 2008).
- [53] C. Domingo-Pardo *et al.* (n_TOF Collaboration), *Phys. Rev. C* **75**, 015806 (2007).
- [54] O. Straniero, R. Gallino, M. Busso, A. Chieffi, C. M. Raiteri, M. Limongi, and M. Salaris, **440**, L85 (1995).
- [55] F. Herwig, *Annu. Rev. Astron. Astrophys.* **43**, 435 (2005), <https://doi.org/10.1146/annurev.astro.43.072103.150600>.
- [56] R. Gallino, C. Arlandini, M. Busso, M. Lugaro, C. Travaglio, O. Straniero, A. Chieffi, and M. Limongi, *Astrophys. J.* **497**, 388 (1998).
- [57] M. Lugaro, A. M. Davis, R. Gallino, M. J. Pellin, O. Straniero, and F. Käppeler, *Astrophys. J.* **593**, 486 (2003).

- 625 [58] T. Rauscher and F.-K. Thielemann, *At. Data. Nucl. Data* 642
626 *Tables* **75**, 1 (2000), arXiv:astro-ph/0004059 [astro-ph]. 643
- 627 [59] C. Ritter, F. Herwig, S. Jones, M. Pignatari, C. Fryer, 644
628 and R. Hirschi, *Mon. Not. R. Astron. Soc.* **480**, 538 645
629 (2018). 646
- 630 [60] B. Paxton, L. Bildsten, A. Dotter, F. Herwig, P. Lesaffre, 647
631 and F. Timmes, *Astrophys. J. Suppl. Ser.* **192**, 3 (2010). 648
- 632 [61] E. Magg *et al.*, *Astron. Astrophys.* **661**, A140 (2022). 649
- 633 [62] M. Asplund, N. Grevesse, A. J. Sauval, and P. Scott, 650
634 *Annu. Rev. Astron. Astrophys.* **47**, 481 (2009), 651
635 <https://doi.org/10.1146/annurev.astro.46.060407.145222>. 652
- 636 [63] E. E. Salpeter, *Astrophys. J.* **121**, 161 (1955). 653
- 637 [64] D. Mascali *et al.*, *Universe* **8**, 10.3390/universe8020080 654
638 (2022). 655
- 639 [65] S. Cristallo, L. Piersanti, O. Straniero, R. Gallino, 656
640 I. Domínguez, C. Abia, G. D. Rico, M. Quintini, and 657
641 S. Bisterzo, *Astrophys. J. Suppl. Ser.* **197**, 17 (2011). 658
- 642 [66] A. I. Karakas and M. Lugaro, *Astrophys. J.* **825**, 26 643
(2016), arXiv:1604.02178 [astro-ph.SR]. 644
- 645 [67] M. Busso, D. Vescovi, S. Palmerini, S. Cristallo, and 646
647 V. Antonuccio-Delogu, *Astrophys. J.* **908**, 55 (2021). 648
- 649 [68] P. Adsley *et al.*, *Phys. Rev. C* **103**, 015805 (2021). 650
- 651 [69] R. Talwar *et al.*, *Phys. Rev. C* **93**, 055803 (2016). 652
- 653 [70] R. Longland, C. Iliadis, and A. I. Karakas, *Phys. Rev. C* 654
655 **85**, 065809 (2012). 656
- 657 [71] Shahina *et al.*, *Phys. Rev. C* **106**, 025805 (2022). 658
- 659 [72] S. Ota *et al.*, *Phys. Rev. C* **104**, 055806 (2021). 660
- 661 [73] H. Jayatissa *et al.*, *Phys. Lett. B* **802**, 135267 (2020). 662
- 663 [74] S. Ota *et al.*, *Phys. Lett. B* **802**, 135256 (2020). 664
- 665 [75] M. Jaeger, R. Kunz, A. Mayer, J. W. Hammer, 666
667 G. Staudt, K. L. Kratz, and B. Pfeiffer, *Phys. Rev. Lett.* 668
669 **87**, 202501 (2001). 670
- 671 [76] M. Wiescher, R. J. deBoer, and J. Görres, *European 672
673 Physical Journal A* **59**, 11 (2023). 674
- 675 [77] D. Rapagnani, C. Ananna, A. Di Leva, G. Imbriani, 676
677 M. Junker, M. Pignatari, and A. Best, *EPJ Web Conf.* 678
679 **260**, 11031 (2022). 680